Article

Potassium Ion Transport by Valinomycin across a Hg-Supported Lipid Bilayer

Lucia Becucci, Maria Rosa Moncelli, Renate Naumann, and Rolando Guidelli

J. Am. Chem. Soc., **2005**, 127 (38), 13316-13323• DOI: 10.1021/ja052920t • Publication Date (Web): 02 September 2005

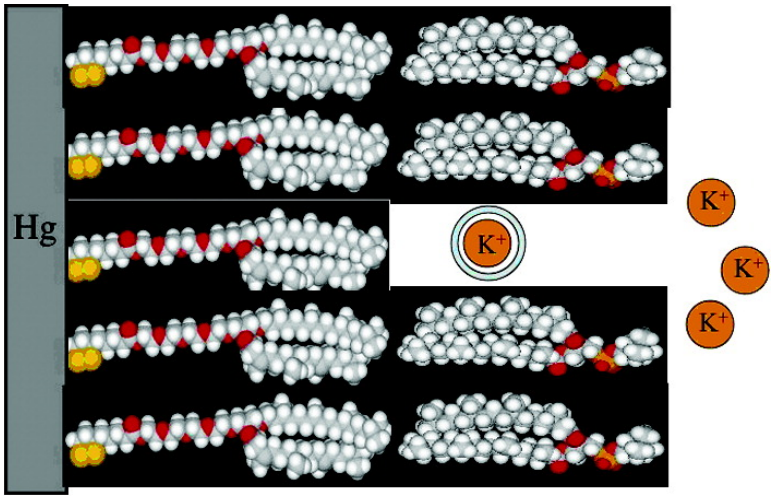

More About This Article

Additional resources and features associated with this article are available within the HTML version:

- Supporting Information
- Links to the 7 articles that cite this article, as of the time of this article download
- Access to high resolution figures
- Links to articles and content related to this article
- Copyright permission to reproduce figures and/or text from this article

View the Full Text HTML

J|A|C|S
ARTICLES
Published on Web 09/02/2005

Potassium Ion Transport by Valinomycin across a Hg-Supported Lipid Bilayer

Lucia Becucci,[†] Maria Rosa Moncelli,[†] Renate Naumann,[‡] and Rolando Guidelli*,[†]

Contribution from the Department of Chemistry, Florence University, Via della Lastruccia 3, 50019 Sesto Fiorentino, Florence, Italy, and Max Planck Institute of Polymer Research, Ackermannweg 10, 55128 Mainz, Germany

Received May 4, 2005; E-mail: rolando.guidelli@unifi.it

Abstract: A biomimetic membrane consisting of a lipid bilayer tethered to a mercury electrode via a hydrophilic spacer was investigated in aqueous KCl by potential-step chronocoulometry and electrochemical impedance spectroscopy, both in the absence and in the presence of the ionophore valinomycin. Impedance spectra, recorded from 1×10^{-2} to 1×10^{5} Hz over a potential range of 0.8 V, are satisfactorily fitted to a series of four RC meshes, which are straightforwardly related to the different substructural elements of the biomimetic membrane. The frequency-independent resistances and conductances of both the lipid bilayer and the hydrophilic spacer show a maximum when plotted against the applied potential. This behavior is interpreted on the basis of a general approximate approach that applies the concepts of impedance spectroscopy to a model of the electrified interphase and to the kinetics of potassium ion transport assisted by valinomycin across the lipid bilayer.

Introduction

The possibility of self-assembling bilayers covalently on metals with formation of rugged functionalized electrodes has stimulated a research aiming at exploiting self-assembly for the realization of biomembrane models capable of incorporating channel-forming peptides and integral proteins in a functionally active state. This has potential not only for fundamental research on protein functions but also for biosensor applications. To achieve this goal, biomimetic membranes consisting of lipid bilayers should be in the liquid crystalline state, they should have a fluidity comparable with that of bilayer lipid membranes (BLMs), they should have water (or, at least, a hydrophilic medium) on both sides of the lipid bilayer, and they should be sufficiently free from pinholes and other defects that might provide preferential pathways for electron and ion transport across the lipid bilayer.[1] The interposition of a hydrophilic layer between a metal and a lipid bilayer is of utmost importance to create the hydrophilic environment required for the proper folding of the extramembrane sections of integral proteins; it is also fundamental to allow a flow of ions across metal-supported lipid bilayers incorporating channel-forming peptides or proteins. With this goal in mind, "thiolipids" consisting of a hydrophilic polyethyleneoxy or oligopeptide chain terminated with a sulfhydryl or disulfide group for anchoring to the metal surface at one end, and covalently linked to the polar head of a lipid molecule at the other end, have been self-assembled on gold[2] or mercury[3] electrodes. The lipid bilayer is formed by self-assembling a further lipid monolayer on top of the tethered thiolipid monolayer, giving rise to a tethered BLM (tBLM). Mercury shares with gold a strong affinity for sulfhydryl groups but has the advantage of being readily renewable and of providing a defect-free surface to the self-assembling film.

This work describes an investigation of potassium ion transport by valinomycin incorporated in a mercury-supported lipid bilayer prepared with a particularly convenient thiolipid (DPTL), recently synthesized in the Max Planck Institute of Polymer Science, Mainz, and used by Naumann et al.[4] for the preparation and characterization of tBLMs on gold. The advantageous features of the present biomimetic membrane are related to the high fluidity of the supported lipid bilayer, thanks to the smooth and liquid surface of mercury, which allows free lateral movement of the tethered thiolipid molecules. This results in electrochemical impedance spectra rich in characteristic features that allow a straightforward fitting to a well-defined

[†] Florence University.
[‡] Max Planck Institute of Polymer Research.

(1) Guidelli, R.; Aloisi, G.; Becucci, L.; Dolfi, A.; Moncelli, M. R.; Tadini Buoninsegni, F. *J. Electroanal.* Chem. **2001**, *504*, 1−28.
(2) (a) Lang, H.; Duschl, C.; Vogel, H. *Langmuir* **1994**, *10*, 197−210. (b) Steinem, C.; Janshoff, A.; von dem Bruch, K.; Reihs, K.; Goossens, J.; Galla, H.-J. *Bioelectrochem. Bioenerg.* **1998**, *45*, 17−26. (c) Cornell, B. A.; Braach-Maksvytis, V. L. B.; King, L. G.; Osman, P. D. J.; Raguse, B.; Wieczorek, L.; Pace R. J. *Nature* **1997**, *387*, 580−583. (d) Naumann, R.; Jonczyk, A.; Kopp, R.; van Esch, J.; Ringsdorf, H.; Knoll, W.; Gräber, P. *Angew. Chem., Int. Ed. Engl.* **1995**, *34*, 2056−2058. (e) Bunjes, N.; Schmidt, E. K.; Jonczyk, A.; Rippmann, F.; Beyer, D.; Ringsdorf, H.; Gräber, P.; Knoll, W.; Naumann, R. *Langmuir* **1997**, *13*, 6188−6194. (f) Heyse, S.; Ernst, O. P.; Dienes, Z.; Hofmann, K. P.; Vogel, H. *Biochemistry* **1998**, *37*, 507−522. (g) Schmidt, E. K.; Liebermann, T.; Kreiter, M.; Jonczyk, A.; Naumann, R.; Offenhausser, A.; Neumann, E.; Kukol, A.; Maelicke, A.; Knoll, W. *Biosens. Bioelectron.* **1998**, *13*, 588−591. (h) Naumann, R.; Schmidt, E. K.; Jonczyk, A.; Fendler, K.; Kadenbach, B.; Liebermann, T.; Offenhäusser, A.; Knoll, W. *Biosens. Bioelectron.* **1999**, *14*, 651−662.
(3) Becucci, L.; Moncelli, M. R.; Guidelli, R. *Langmuir* **2003**, *19*, 3386-3392.
(4) (a) Naumann, R.; Schiller, S. M.; Gie*β*, F.; Grohe, B.; Hartman, K. B.; Kärcher, I.; Köper, I.; Lübben, J.; Vasilev, K.; Knoll, W. *Langmuir* **2003**, *19*, 5435−5443. (b) Naumann, R.; Walz, D.; Schiller, S. M.; Knoll, W. *J. Electroanal. Chem.* **2003**, *550*−*551*, 241−247. (c) Schiller, S. M.; Naumann, R.; Lovejoy, K.; Kunz, H.; Knoll, W. *Angew. Chem., Int. Ed.* **2003**, *42*, 208−211.

10.1021/ja052920t CCC: $30.25

equivalent circuit, thus providing a wealth of information on the structure of this biomimetic membrane and on the effect of the incorporation of ionophores. Impedance spectra of this mercury-supported tBLM were recorded over a broad potential range, thus allowing the estimate of the potential dependence of a number of circuit elements that, due to the excellent fitting to the equivalent circuit over a frequency range from 10^{-2} to 10^5 Hz, can be regarded as frequency-independent. The potential-dependence of the above circuit elements is explained by a novel general approach based on a model of the electrified interface.

Materials and Methods

The water used was obtained from water produced by an inverted osmosis unit, upon distilling it once and then distilling the water so obtained from alkaline permanganate. Merck suprapur KCl was baked at 500 °C before use to remove any organic impurities. Diphytanoylphosphatidylcholine (DphyPC) was purchased from Avanti Polar Lipids (Birmingham, AL). Valinomycin (VM) was purchased from Sigma and used without further purification. The 2,3,di-*O*-phytanyl-*sn*-glycerol-1-tetraethylene-glycol-D,L-α lipoic acid ester lipid (DPTL) was obtained from the Max Planck Institute for Polymer Research in Mainz. It consists of a tetraethyleneoxy (TEO) chain covalently linked to a lipoic acid residue for anchoring to the metal at one end and bound via ether linkages to two phytanyl chains at the other end. The other chemicals and solvents were commercially available and used as received.

DphyPC solutions were prepared by diluting a proper amount of stock solution of this phospholipid with pentane. Solutions of 0.2 mg/mL DPTL in ethanol were prepared from a 2 mg/mL solution of DPTL in ethanol. Stock solutions of this thiolipid were stored at −18° C. Stock solutions of 3.6×10^{-4} M VM were prepared in ethanol and stored at +4° C.

All measurements were carried out in aqueous 0.1 M KCl, unless otherwise stated. A homemade hanging mercury drop electrode (HMDE), described elsewhere,[5] was employed. Use was made of a homemade glass capillary with a finely tapered tip, about 1 mm in outer diameter. Capillary and mercury reservoir were thermostated at 25 ± 0.1 °C by the use of a water-jacketed box to avoid any changes in drop area due to a change in temperature. One glass electrolysis cell containing the aqueous solution and a small glass vessel containing the ethanol solution of the thiolipid were placed on a movable support inside the box.[6] The HMDE and the support were moved vertically and horizontally, respectively, by means of two oleodynamic systems that ensured the complete absence of vibrations.

AC voltammetry, chronocoulometry, and impedance spectroscopy measurements were carried out with an Autolab instrument (Echo Chemie) supplied with an FRA2 module for impedance measurements, an SCAN-GEN scan generator, and GPES 4.9 software. Potentials were measured versus a Ag|AgCl electrode immersed in the KCl working solution but are referred to a saturated calomel electrode (SCE). Charge versus time curves recorded analogically for long time periods by the chronocoulometric technique were affected by an appreciable offset charge varying linearly in time, which was subtracted from these curves.

Monolayers of DPTL were self-assembled on the HMDE by keeping the mercury drop immersed in the small vessel containing the thiolipid solution for 20 min. In the meantime, a pentane solution of DphyPC was spread on the surface of the aqueous solution in the glass cell, in an amount corresponding to five to six phospholipid monolayers, and the pentane was allowed to evaporate. Using the oleodynamic system, the DPTL-coated HMDE was then extracted from the vessel, washed with ethanol to remove the excess of adsorbed thiolipid, and kept in a N_2 atmosphere for the time strictly necessary to allow the solvent to evaporate. Immediately afterward, the electrolysis cell containing the aqueous solution on whose surface DphyPC had been previously spread was brought below the HMDE, and the latter was lowered so as to immerse it into the aqueous solution across the phospholipid film; this procedure causes a DphyPC monolayer to self-assemble on top of the DPTL monolayer, thanks to the hydrophobic interactions between the alkyl chains of the phospholipid and those of the thiolipid. These interactions cause these chains to come into contact, giving rise to a lipid bilayer interposed between the hydrophilic moiety of the thiolipid and the aqueous solution. The applied potential was then repeatedly scanned over a potential range from −0.200 to −1.200 V while continuously monitoring the curve of the quadrature component, *Y*", of the electrode admittance at 75 Hz against the applied potential, *E*, using AC voltammetry, until a stable *Y*" versus *E* curve was attained (incidentally, in aqueous 0.1 KCl, bare mercury starts to be oxidized at potentials positive of 0.00 V, DPTL-coated mercury at potentials positive of +0.100 V). The minimum Y"/ω value for the resulting DPTL|DphyPC-coated mercury, where ω is the angular frequency, ranged from 0.55 to 0.65 μF cm^{-2}. This quantity, which provides a rough measure of the differential capacity of the tBLM, is somewhat less than the capacity, ∼0.8−0.9 μF cm^{-2}, of a solvent-free black lipid membrane.[7] VM was incorporated in this tBLM by simply adding its stock solution to the electrolysis cell in an amount corresponding to 1.5×10^{-7} M. The solution was, then, stirred for a few minutes, while keeping the electrode at an applied potential of −0.500 V, at which VM shuttles K^+ ions across the lipid bilayer.

Each set of measurements over the whole accessible potential range was repeated at least five times on different tBLMs. Deviations of the directly measured in-phase and quadrature components of the impedance from their average values, over the whole set of different tBLMs employed, were less than 10%. However, due to the propagation of errors in the fitting of the raw impedance data to an equivalent circuit consisting of four RC meshes, the four *R* and *C* values resulting from the fitting were found to exhibit average percentage errors as high as 40%, when estimated over the whole set of tBLMs. Within a set of impedance spectra obtained on a single tBLM in the presence of VM, the *R* and *C* values relative to the lipoic acid residue, the TEO moiety, and the lipid bilayer exhibited average percentage errors less than 3%; the *R* and *C* values relative to the aqueous solution adjacent to the tBLM showed somewhat higher average percentage errors, due to the narrow range of accessible high frequencies over which the solution controls the impedance.

Results

Curve *a* in Figure 1 is a plot of the charge *Q* versus time *t* obtained on a newly formed tBLM immersed in aqueous 0.1 M KCl by performing a potential step from −0.200 V to −1.050 V. After an initial abrupt increase in charge, due to the flow of the capacitive current required to charge the tBLM, the curve assumes a sigmoidal shape tending to a constant limiting value. If we step the potential back to −0.200 V and, immediately afterward, we carry out a further potential step to −1.050 V, only the initial abrupt increase in charge is observed, after which the charge remains constant in time. The pristine curve *a* is recovered by keeping the electrode at −0.200 V for about 10 min before performing the potential step to −1.050 V. By adopting a rest time of 10 min at −0.200 V before each negative potential step, a slow increase of charge in time, beyond the initial abrupt increase due to the capacitive current, starts to be observed at final potentials E_f negative of −0.800 V (data not shown). The more the potential is shifted in the negative direction, the more the increase in charge is observed at shortened times, until the *Q* versus *t* curves assume a sigmoidal

(5) Moncelli, M. R.; Becucci, L. *J. Electroanal. Chem.* **1997**, *433*, 91−96.
(6) Tadini Buoninsegni, F.; Herrero, R.; Moncelli, M. R. *J. Electroanal. Chem.* **1998**, *452*, 33−42.
(7) Montal, M.; Mueller, P. *Proc. Natl. Acad. Sci. U.S.A.*, **1972**, *69*, 3561−3566.

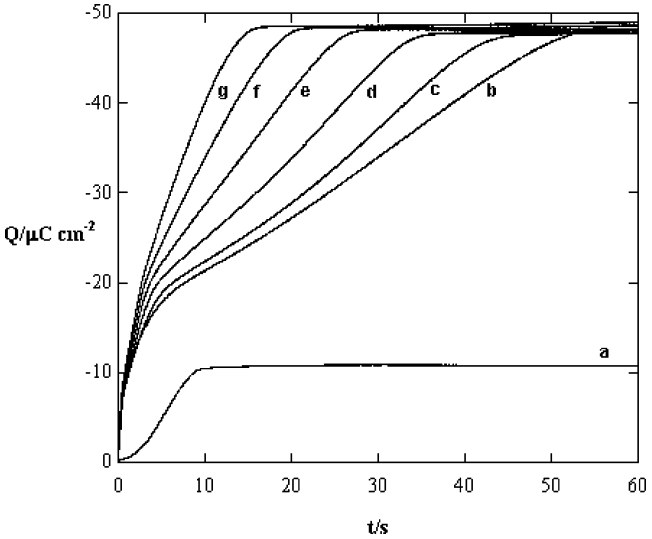

Figure 1. Curve a is a charge versus time curve at a tBLM in 0.1 M KCl following a potential step from −0.200 V to −1.050 V. The other curves were obtained at a tBLM in 0.1 M KCl and 1.5×10^{-7} M VM, following potential steps from $E_i = -0.200$ V to E_f values decreasing from −0.800 V (b) to −1.050 V (g) by 50 mV decrements. Each potential step was preceded by a rest time of 10 min at $E_i = -0.200$ V.

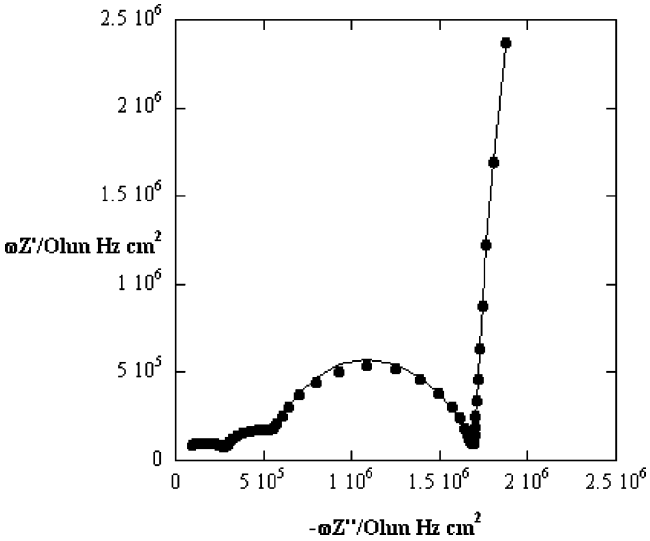

Figure 2. Plot of $\omega Z'$ versus $\omega Z''$ at a tBLM in 0.1 M KCl and 1.5×10^{-7} M VM, recorded at −0.41 V.

shape over the selected time range and attain the maximum value shown by curve *a* in Figure 1. The height of the sigmoidal curve *a* in Figure 1, after subtracting the small initial abrupt increase, amounts to about 10 μC cm^{-2}. The fact that this charge is not recovered, when short rest times at −0.200 V are adopted, indicates that it is due to some conformational change of the TEO moiety at potentials negative of −0.800 V and that the conformation stable at −0.200 V can be restored only slowly. The sigmoidal shape of curve *a* in Figure 1 strongly suggests that this conformational change is of a cooperative nature and proceeds via a nucleation-and-growth mechanism.[8] The height of this curve provides the charge involved in the conformational change. Preliminary measurements with the present tBLM showed that the dipole potential of the TEO moiety amounts to about −250 mV, negative toward the metal.[9] The conformational change taking place gradually as we proceed toward more negative potentials is expected to progressively shift this dipole potential toward less negative values.

Curves *b* to *g* in Figure 1 are *Q* versus *t* curves obtained at a tBLM incorporating VM from its 1.5×10^{-7} M aqueous solution, by performing a series of potential steps from $E_i = -0.200$ V to E_f values ranging from −0.800 to −1.050 V. Each potential step was preceded by a rest time of 10 min at E_i. The charge increases in time with two distinct slopes and then attains a plateau. The plateau is attained at shorter times as E_f is made more negative. The height of the plateau amounts to about 40 μC cm^{-2}, after subtracting the charge involved in the conformational change of the TEO moiety. It can be regarded as the maximum charge of potassium ions that can be accommodated in the hydrophilic TEO moiety in the conformational state stable at the more negative potentials.

Figure 2 shows a plot of $\omega Z'$ versus $\omega Z''$ for a tBLM incorporating VM from its 1.5×10^{-7} M solution in 0.1 M KCl, at a potential of −0.410 V at which it shuttles K^+ across the lipid bilayer; ω is the angular frequency, and Z', Z'' are the in-phase and quadrature components of the impedance

Four partially fused semicircles are clearly visible. In a $\omega Z'$ versus $\omega Z''$ plot, a semicircle corresponds to an *RC* mesh; the diameter of the semicircle measures the reciprocal, 1/*C*, of the capacity of the *RC* mesh, while the ω value at the maximum of the semicircle measures the reciprocal of its time constant, $\tau = RC$. The frequency increases in the direction of increasing $\omega Z''$. Therefore, the time constants of the RC meshes in Figure 2 decrease as we proceed along the $\omega Z''$ axis. Let us denote the meshes by the numbers 1 to 4 in the order of increasing frequency. The solid curve in the figure is the best fit of the plot to an equivalent circuit consisting of a series of four *RC* meshes. The fitting is quite satisfactory at all potentials over the range from −0.200 to −1.000 V, with average percentage errors less than 3%; consequently, it yields circuit elements that are practically independent of the frequency ω but depend on the applied potential *E*.

Figures 3 and 4 show plots of the capacities and conductances of the intermediate meshes 2 and 3 in the presence of VM against the applied potential *E*, as obtained upon subtracting the corresponding quantities in the absence of VM. This allows a direct comparison of these curves with those calculated in the following, upon estimating exclusively the contribution to these quantities from the progressive flow of potassium ions into the tBLM with a negative shift in the applied potential. The quantities in Figures 3 and 4 will be overbarred to distinguish them from the capacities and conductances obtained in the absence of VM. It is apparent that both the capacity $\bar{C}_2$ and the conductance $\bar{g}_2 \equiv 1/\bar{R}_2$ of mesh 2 show maxima in the proximity of −0.800 V, while those, $\bar{C}_3$ and $\bar{g}_3 \equiv 1/\bar{R}_3$, of mesh 3 show maxima at about −0.400 V. The above data were obtained by recording the impedance spectra from −0.300 to −1.000 V by −25 mV increments. During this recording, the TEO moiety is expected to undergo a gradual conformational change accompanied by a progressive decrease in its negative dipole potential. To point out the effect of this change, impedance spectra were also recorded upon keeping the electrode at a rest potential of −0.250 V for 8 s before measuring

(8) Becucci, L.; Moncelli, M. R.; Guidelli, R. *J. Am. Chem. Soc.* **2003**, *125*, 3785−3792.
(9) Moncelli, M. R.; Becucci, L.; Schiller, S. M. *Bioelectrochemistry*, **2004**, *63*, 161−167.

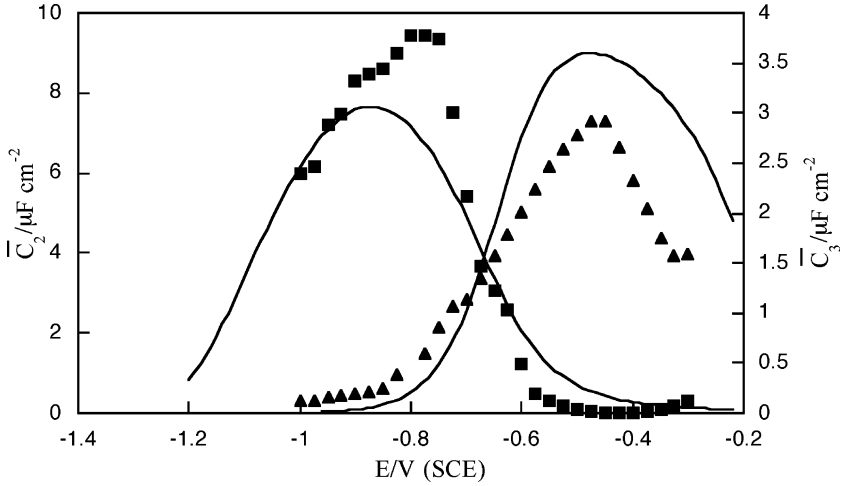

Figure 3. Plots of $\bar{C}_2$ (solid squares) and $\bar{C}_3$ (solid triangles) against E at a tBLM in 0.1 M KCl and 1.5×10^{-7} M VM. The solid curves are best fits obtained for $K_3 = 5 \times 10^{-3}$, $K_2 = 3 \times 10^5$ cm^3 mol^{-1}, $C_1 = 4\ \mu$F cm^{-2}, $C_3 = 7\ \mu$F cm^{-2}, $C_2 = 1\ \mu$F cm^{-2}, $\chi_3 = -0.250$ V, and $\Gamma_m = 1 \times 10^{-11}$ mol cm^{-2}.

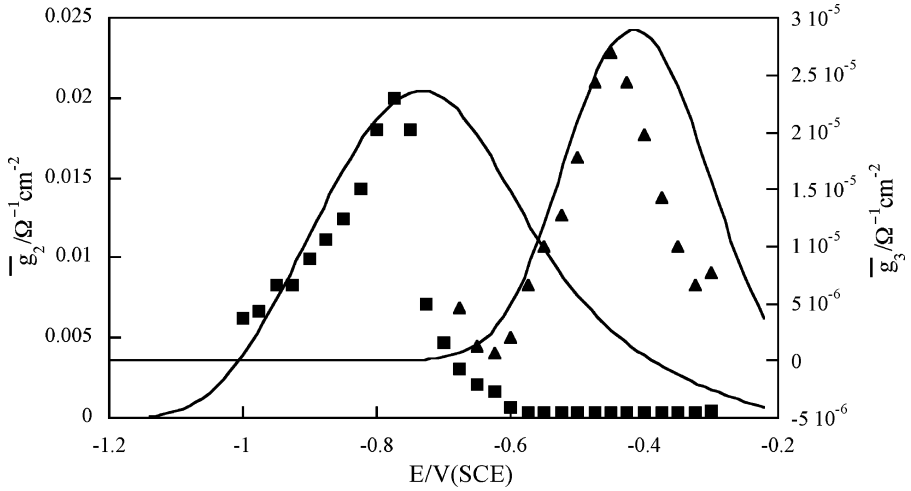

Figure 4. Plots of $\bar{g}_2$ (■) and $\bar{g}_3$ (▲) against E at a tBLM in 0.1 M KCl and 1.5×10^{-7} M VM. The solid curves are best fits obtained for the same parameters as those in Figure 3 and for $\alpha = 0.5$, $k_{3,b} = 4 \times 10^{16}$ cm^2 s^{-1} mol^{-1}, and $k_{2,b} = 15$ s^{-1}.

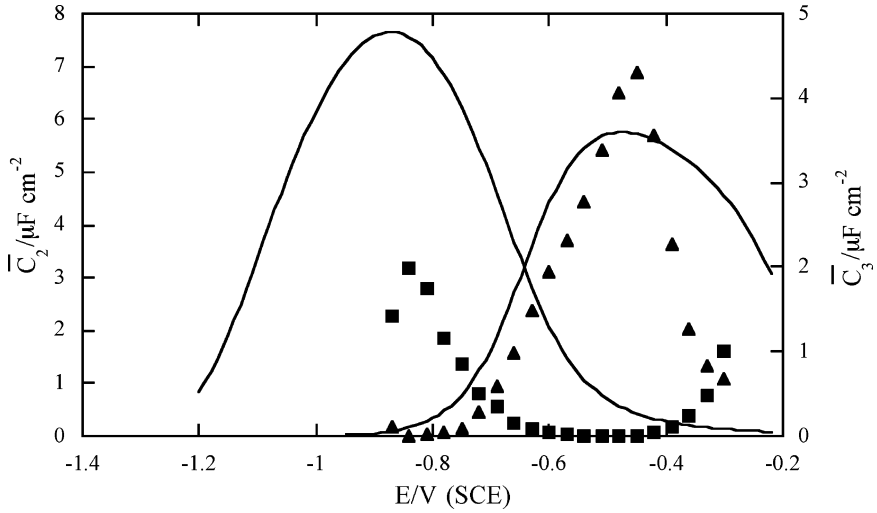

Figure 5. Plots of $\bar{C}_2$ (solid squares) and $\bar{C}_3$ (solid triangles) against E at a tBLM in 0.1 M KCl and 1.5×10^{-7} M VM, as obtained upon pretreating the electrode at -0.250 V. The solid curves are the same as those in Figure 3.

the electrode impedance at each frequency and at each applied potential, in an attempt to maintain the TEO conformation that is stable at the less negative potentials even during measurements at the more negative ones. Figure 5 shows plots of $\bar{C}_2$ and $\bar{C}_3$ against E obtained upon pretreating the electrode at -0.250 V.

Even though $\omega Z'$ versus $\omega Z''$ plots at a tBLM in the absence of VM do not exhibit features as distinguishable as of those observed in its presence, these plots are still satisfactorily fitted

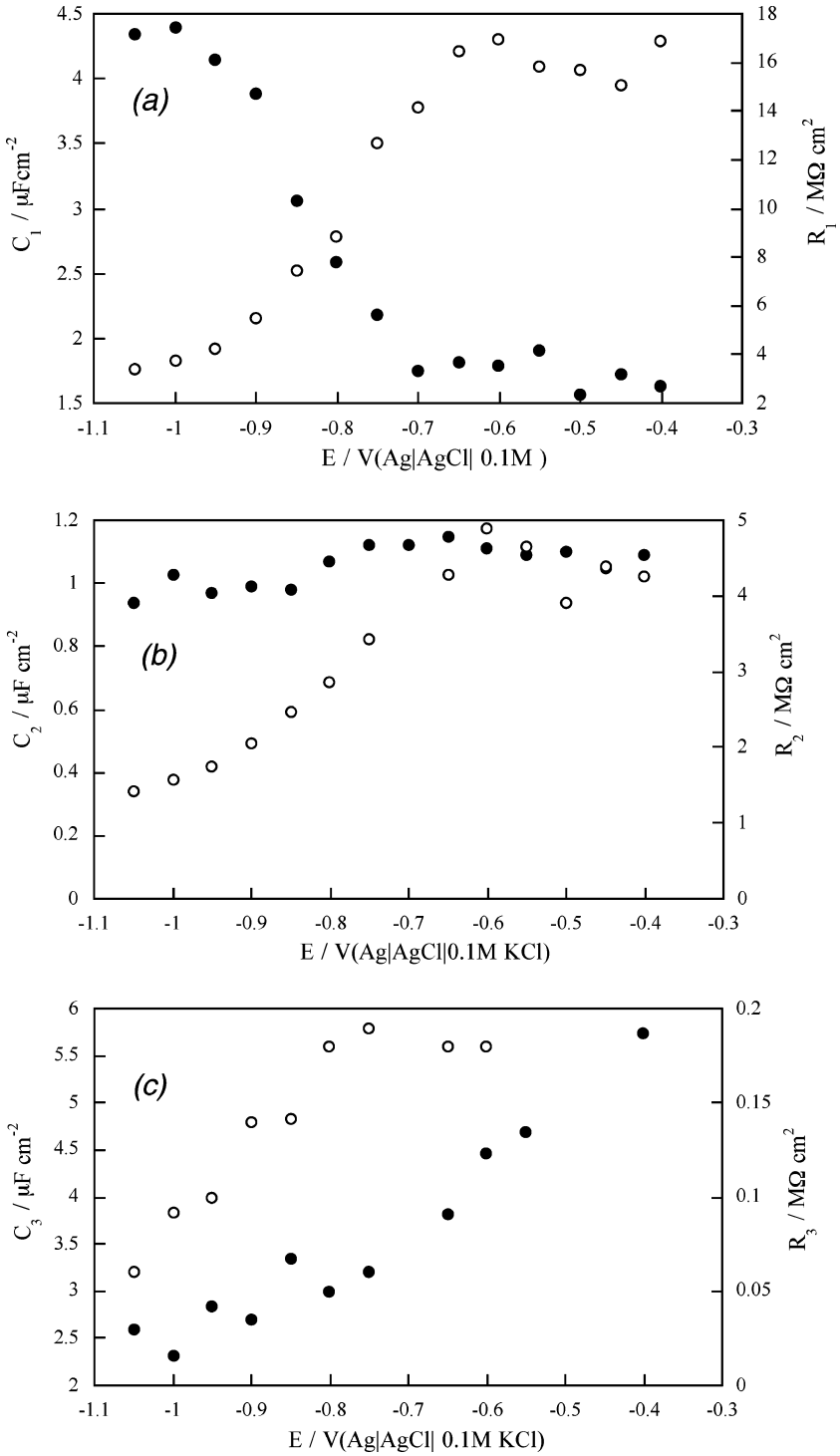

Figure 6. Plots of C_1 and R_1 (a), C_2 and R_2 (b), and C_3 and R_3 (c) against E at a tBLM in 0.1 M KCl. C values are represented by solid circles, R values by open circles.

to a series of four *RC* meshes, with average percentage errors usually less than 20%. Impedance spectra measured in KCl aqueous solutions of concentrations ranging from 5×10^{-3} to 0.1 M yield R and C values for the first three meshes that are practically independent of the electrolyte concentration. Figures 6a, 6b, and 6c show plots of the capacities and resistances of these three meshes against potential. On the other hand, $g_4 \equiv 1/R_4$ and C_4 are practically proportional to the KCl concentration, as shown in Figure 7. The proportionality of g_4 to the electrolyte concentration clearly indicates that mesh 4 is to be ascribed to the aqueous solution bathing the biomimetic membrane. The corresponding capacity C_4 being proportional to the KCl concentration is due to the progressive decrease in the ohmic drop between the mercury electrode and the counter-electrode. The other meshes being unaffected by the electrolyte concentration indicates that K^+ ions cannot penetrate the membrane in the absence of the ionophore. Results substantially analogous to those reported in Figures 6 and 7 were obtained at a tBLM immersed in an aqueous solution of 0.1 M tetramethylammonium chloride and 1.5×10^{-7} M VM. This indicates that the

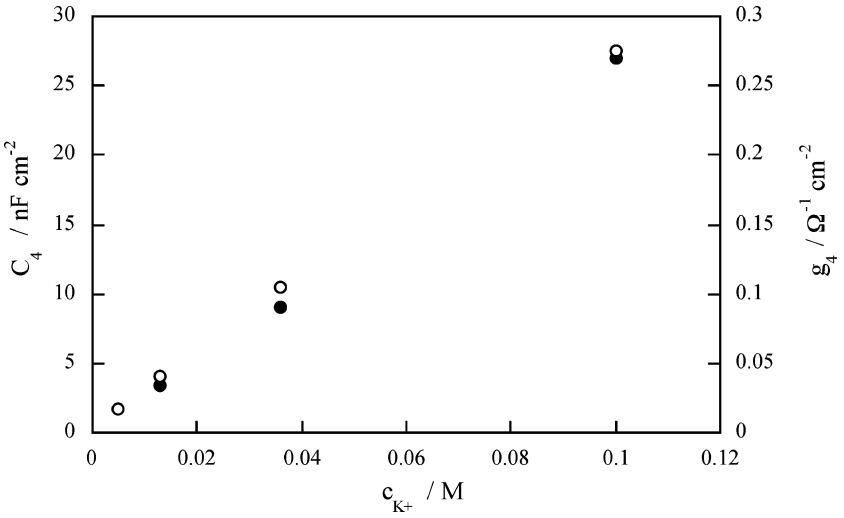

Figure 7. Plots of g_4 (○) and C_4 (●) at a tBLM in 0.1 M KCl against the potassium ion concentration.

incorporation of VM does not disorganize the lipid bilayer to such an extent as to form pores allowing the nonspecific translocation of tetramethylammonium ions across the bilayer.

Discussion

The four *RC* meshes must be related to different portions of the tBLM. In fact, the electrified interface consisting of the thiolipid monolayer tethered to the mercury surface, with a phospholipid monolayer on top of it and the adjacent aqueous solution, is a heterogeneous system with a substructure in which the dielectric and/or conductance properties of the substructural elements are different. This gives rise to a dispersion of the impedance with frequency, due to interfacial polarization at the substructural-element interfaces, which provides a means of detecting and characterizing these dielectric slabs. In an equivalent circuit, each slab can be represented by an R_iC_i mesh, with all meshes being in series with each other. Some of these meshes may be either prevalently resistive, with a very small capacitive element, or else prevalently capacitive, with a very high resistive element. Thus, the mesh representing the aqueous solution adjacent to the lipid bilayer is mainly resistive. Conversely, the mesh representing the dielectric slab immediately adjacent to the blocking mercury electrode is expected to be mainly capacitive.

Before ascribing the four *RC* meshes in the presence of VM to different slabs, it is convenient to examine the impedance spectra of the tBLM in the absence of VM, and hence in the absence of K^+ transport. The capacity C_2 is potential-independent (see Figure 6), and its value, about 1 μF cm^{-2}, is close to that of solvent-free BLMs;[7] it is therefore reasonable to ascribe mesh 2 to the lipid-bilayer moiety of the membrane. The resistance R_2 is practically constant and about equal to 4−5 MΩ cm^2 at potentials positive of about −0.700 V but decreases at more negative potentials. This denotes a slight leakage of ions across the lipid bilayer at these negative potentials. The capacity C_3 decreases roughly linearly from 6 to 2 μF cm^{-2} with a negative shift in E. The C_3 value of 6 μF cm^{-2} is not too far from that, 10 μF cm^{-2}, for a triethyleneoxythiol self-assembled monolayer on mercury in direct contact with an aqueous solution.[10] Mesh 3 can, therefore, be reasonably ascribed to the TEO moiety of the biomimetic membrane. It has been reported that this moiety is present in a rather hydrophobic helical structure.[11] The decrease of C_3 with a negative shift in potential can be explained by a progressive elongation of this moiety under the influence of a local electric field increasingly directed toward the metal. The increase in the length of the TEO moiety does not involve an increase in its resistance R_3, as one would expect on the basis of Ohm laws; conversely, R_3 decreases, suggesting that the increase in the volume of the hydrophilic region increases its capability of accommodating water molecules and protons. Mesh 1 is characterized by the highest values of the resistance. Thus, R_1 decreases from 16 to about 4 MΩ cm^2 with a negative shift in E, while the corresponding capacity, C_1, increases from 2 to 4.5 μF cm^{-2}, as expected. The very high R_1 values of mesh 1 suggest that the dielectric slab responsible for this mesh is the one immediately adjacent to the blocking mercury surface, namely the lipoic acid moiety. As a matter of fact, for a dielectric slab to have a finite resistance, the charges flowing across it should be in a condition of being accommodated on both sides of the slab. However, the electrode surface is not completely blocking, since the solution will normally contain trace impurities of charged species that may be strongly adsorbed on the electrode surface, competing with the thiolipid. Consequently, even the slab adjacent to the electrode surface has a measurable resistance, albeit very high. Further evidence in favor of this conclusion is provided by the increase in capacity and decrease in resistance of this slab with an increase in the local electric field directed toward the mercury surface. The elongation of the TEO moiety by this field may increase the electrostatic pressure upon the lipoic acid hydrocarbon chains, causing their progressive tilt. This will, in turn, decrease the thickness of the lipoic acid moiety, with a resulting increase in capacity and decrease in resistance. Incidentally, the thickness l of the lipoic acid moiety in its more extended conformation, as estimated from a space-filling model, amounts to about 9 Å; upon setting the dielectric constant ϵ of the hydrocarbon chains of the lipoic acid equal to that, 2, of decane, the Helmholtz formula, $C = \epsilon/(4\pi l)$, yields a capacity of 2 μF cm^{-2}, in good agreement with the experimental value at the less negative potentials.

(10) Becucci, L.; Guidelli, R.; Liu, Q.; Bushby, R. J.; Evans, S. D. *J. Phys. Chem. B* **2002**, *106*, 10410−10416.
(11) Zolk, M.; Eisert, F.; Pipper, J.; Herrwerth, S.; Eck, W.; Buck, M.; Grunze, M. *Langmuir* **2000**, *16*, 5849−5852.

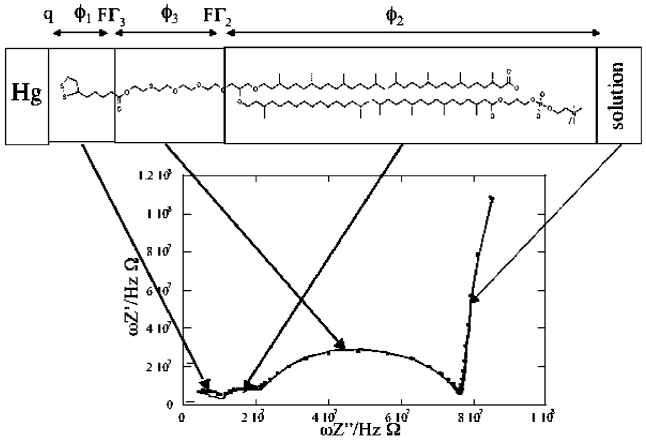

Figure 8. Representation of the correlation between the semicircles of the $\omega Z'$ versus $\omega Z''$ plot and the different substructural elements of the tBLM. The location of the charges and the potential differences across the different dielectric slabs are reported on top of the figure.

In practice, the lipoic acid residue behaves like a pure capacitive element and the aqueous solution behaves like a pure resistive element, both in the absence and in the presence of VM. Therefore, in examining the impedance spectra in the presence of VM, attention will only be focused on the R and C values of meshes 2 and 3, corresponding to the lipid bilayer and to the TEO moiety (see Figure 8). In the presence of 1.5×10^{-7} M VM these quantities depend strongly upon the applied potential E, as shown in Figures 3 and 4. In fact, $\bar{C}_2$, $\bar{g}_2 = 1/\bar{R}_2$ and $\bar{C}_3$, $\bar{g}_3 = 1/\bar{R}_3$ account for the gradual accumulation of K^+ ions in the corresponding slabs as the potential is progressively shifted in the negative direction.

Even though K^+ ions are distributed in space across the biomimetic membrane, albeit nonhomogeneously, the ideal circuit elements used for the fitting represent ideal lumped-constant properties.

In view of the above choice of substructural elements, the charges will be assumed to be located as follows (see Figure 8): a free electronic charge density q on the surface of the mercury electrode, a charge density $F\Gamma_3$ at the boundary between the lipoic acid residue and the TEO moiety, and a charge density $F\Gamma_2$ at the boundary between the TEO moiety and the lipid bilayer. Here, Γ_3 and Γ_2 are surface concentrations of K^+ ions. With this charge distribution, the extrathermodynamic absolute potential difference ϕ_t across the whole interphase, which is more positive than the potential E measured versus a SCE by about 0.250 V at a mercury|aqueous solution interphase,[3] is given by

$$\phi_t \cong E(\mathrm{SCE}) + 0.250\ \mathrm{V} = \frac{q}{C_1} + \left(\frac{q + F\Gamma_3}{C_3} + \chi_3\right) + \frac{q + F(\Gamma_3 + \Gamma_2)}{C_2} \equiv \phi_1 + \phi_3 + \phi_2 \quad (1)$$

Here, C_1, C_3, and C_2 are the "intrinsic" capacities obtained in the absence of VM; ϕ_1, ϕ_3, and ϕ_2 are, in this order, the potential difference across the lipoic acid moiety, across the TEO moiety, and across the lipid bilayer; ϕ_3 includes the dipole potential, χ_3, of the TEO moiety, which was estimated at about -0.250 V, negative toward the metal, on the basis of independent measurements.[9] As a matter of fact, K^+ ions are expected to be distributed along the whole TEO hydrophilic spacer. More precisely, in view of the preference of K^+ ions to reside close to the oxygen of each ethyleneoxy monomeric unity, each of these units may be represented by a single RC mesh. From the point of view of circuit analysis, a series of n identical RC meshes is equivalent to a single mesh, with a resistance equal to nR and a capacitance equal to C/n. The use of a single R_3C_3 mesh for the TEO moiety is, therefore, justified.

The fitting program regards the parameters $\bar{C}_2$, $\bar{g}_2$ and $\bar{C}_3$, $\bar{g}_3$ as frequency-independent and independent of each other along each impedance spectrum at constant E, albeit allowing for their variation with a change in E, due to their dependence on Γ_2 an Γ_3. For the R_iC_i mesh associated to any given dielectric slab to satisfy this condition, use is made of the general approximate approach outlined in the Supporting Information (SI) file available on the Web. The reference numbers of the equations reported in the SI file are preceded by the letter A, which stands for Appendix.

Suffice here to summarize the main assumptions made in this approach. The small perturbation, Δj, in the current that flows to and fro in any of the two dielectric slabs representing the TEO moiety and the lipid bilayer, and that charges and discharges the two boundaries of the corresponding slab, is set equal to the time derivative of the perturbation, $F\Delta\Gamma$, in the charge on the metal side of the slab (eq A1). Moreover, in view of the small a.c. perturbation, ΔE, in the applied potential, Δj is regarded as a linear function of both $\Delta\Gamma$ and ΔE (eq A2). The current, j_2, flowing along the lipid bilayer moiety and requiring K^+ ions to surmount the corresponding potential energy barrier is expressed by a Butler−Volmer-like equation (eq A6), where $k_{2,f}$ and $k_{2,b}$ are the corresponding forward and backward rate constants for $\phi_2 = 0$. Under equilibrium conditions, namely for $j_2 = 0$, this equation reduces to a Langmuir isotherm, with a potential-independent adsorption equilibrium constant $K_2 = k_{2,f}/k_{2,b}$ (eq A7). An analogous Butler−Volmer-like equation is used to express the current, j_3, due to the translocation of K^+ ions across the TEO moiety (eq A8), where $k_{3,f}$ and $k_{3,b}$ are the corresponding forward and backward rate constants for $\phi_3 = 0$ and $K_3 = k_{3,f}/k_{3,b}$ is the corresponding adsorption equilibrium constant.

The solid curves in Figures 3 and 4 are plots of $\bar{C}_2$, $\bar{C}_3$ and $\bar{g}_2$, $\bar{g}_3$ versus potential, calculated on the basis of the approach outlined in the appendix. The parameters employed are reported in the legends. Agreement between experimental plots and calculated curves is semiquantitative. The C_1, C_2, and C_3 values used for the fitting are either very close or practically coincident with those estimated from the impedance spectra in the absence of VM (see Figure 6). On the other hand, the Γ_m value used for the fitting, which corresponds to a charge density of about 1 μC cm^{-2}, bears no direct relation to the maximum charge of 40 μC cm^{-2} estimated from Figure 1, for the following reason. A realistic distribution of K^+ ions throughout the whole hydrophilic spacer can be formally accounted for by a series of an unknown number, m, of identical RC meshes of capacity $\bar{C}_m$; the overall capacity of this series is equal to $\bar{C}_m/m$. Consequently, the $(\Delta\Gamma_i)/(\Delta E)$ ratio in eq A5b and $\partial\Gamma_i/\partial E$ in eq A4b are also divided by m, and the same is true for Γ_m.

The calculated plots of $\bar{C}_2$ and $\bar{C}_3$ against E depend only on the parameters K_2 and K_3 and on the maximum concentration of K^+ ions in the TEO moiety, Γ_m, while those of $\bar{g}_2$ and $\bar{g}_3$

against E also depend on $k_{2,b}$ and $k_{3,b}$. The fact that the quantities $\bar{C}_3$ and $\bar{g}_3$, relative to the TEO moiety, attain a maximum at less negative potentials than the quantities $\bar{C}_2$ and $\bar{g}_2$, relative to the lipid bilayer, is due to the negative dipole potential, χ_3, located in the TEO moiety, which favors an incipient accumulation of K^+ ions on the metal side of the hydrophilic spacer. On the other hand, the height of the potential energy barrier due to the lipid bilayer decreasing toward more negative potentials causes the conductance $\bar{g}_2$, which is responsible for the accumulation of K^+ on the solution side of the TEO moiety, to be greater than $\bar{g}_3$.

A pretreatment of the electrode at -0.250 V before each impedance measurement causes the $\bar{C}_2$ versus E peak to be much lower than that obtained without pretreatment, as appears by comparing Figures 5 and 3. Thus, the peak in Figure 5 is much lower than that calculated on the basis of the same parameters as those employed in Figure 3. This indicates that forcing the TEO moiety to be in the shrunk conformation (stable at less negative potentials) at the more negative potentials at which it should be in the elongated one decreases its capability of accumulating K^+ ions on the solution side of the TEO moiety, with a resulting decrease in capacity; conversely, the $\bar{C}_3$ versus E peak is only slightly varied, because of the electrostatic attraction exerted on the K^+ ions by the negative dipole potential of the TEO moiety.

In conclusion, it has been shown that a biomimetic membrane consisting of a bilayer tethered to mercury via a hydrophilic spacer may provide a wealth of information on the structure of the membrane and on the effect of the incorporation of ion carriers in the bilayer, when impedance spectra are recorded over a broad potential range. This is mainly due to the smoothness and fluidity of the liquid mercury surface. The different substructural elements of the membrane are characterized by different *RC* meshes in series with each other. The potential dependence of the resulting circuit elements can be related to the structure of the membrane and to the gradual filling of the hydrophilic spacer by ions shuttled by an ion carrier, on the basis of a general approximate approach. Application of the present technique to the channel-forming peptides gramicidin and melittin and to the channel-forming protein OmpF, the best known porin of *Escherichia coli*, is in progress.

Acknowledgment. Thanks are due to MIUR (Ministry of Education, University and Research) of Italy for financial support through the Grant PRIN 2003 035241 and to Ente Cassa di Risparmio di Firenze for financial support through the PROMELAB project.

Supporting Information Available: A general approximate approach, which applies the concepts of impedance spectroscopy to a model of the electrified interphase and to the kinetics of potassium ion transport assisted by VM across the tBLM, is contained in a Supporting Information (SI) file. This material is available free of charge via the Internet at http://pubs.acs.org.

JA052920T